Journal of Chemical Health Risks

www.jchr.org

JCHR (2025) 15(6), 3739-3745 | ISSN:2251-6727

Green Synthesis of $Ce_2Zr_2O_7$ Nanocomposite for the Photocatalytic Application

Kovendhan S [1] and Sheela R [2*]

[1]Research Scholar, Department of Civil Engineering Annamalai University, Annamalai Nagar, Chidambaram Tamilnadu, India

[2*]Associate Professor, Department of Civil Engineering Annamalai University, Annamalai Nagar, Chidambaram Tamilnadu, India

(Received: 19 October 2025 Revised: 28 October 2025 Accepted: 23 November 2025)

KEYWORDS

Green synthesis, Activated carbon, Methylene blue dye and environmental remediation.

ABSTRACT:

To synthesis Ce based ZrO nanocomposites via., green synthesis method. The synthesized activated carbon ZrO_2, AC/$Ce_2Zr_2O_7$ were characterized various analytical techniques such as XRD, FT-IR, SEM-EDS and UV-DRS. The crystalline sizes of the synthesized activated carbon ZrO2, AC/$Ce_2Zr_2O_7$ are 24.2, 29.4 and 36.7 nm, respectively. The morphologies of prepared materials were investigated using SEM, it was discovered that Activated carbon, ZrO_2, AC/$Ce_2Zr_2O_7$ nanocomposite showed sheet, agglomerated and spherical shapes. UV-DRS analysis is used to determine the bandgap of the synthesized activated carbon ZrO_2, AC/$Ce_2Zr_2O_7$ was found to be 3.7 and 3.4 eV, respectively. The materials were used as a catalyst for the photodegrading of methylene blue dye and the AC/$Ce_2Zr_2O_7$ material highly degrading the dye molecules up to 88.2%.

Introduction

In recent years, environmental contamination has grown to be a major problem. Pollution levels are rising daily, causing major and irreversible damage to the planet. It has been shown that the primary source of water contamination is industrial effluent. Photocatalytic degradation is a crucial stage in the treatment of wastewater that may get rid of hazardous heavy organic pollutants. The drawbacks of conventional wastewater treatment applications include high separation costs and the secondary generation of pollutants related to adsorption, clotting, and membrane separation all of which have significant operational costs. When present, metal oxide nanocomposites promote photocatalytic degradation[1]. activated carbon, ZrO_2, AC/$Ce_2Zr_2O_7$ nanostructures are of interest to researchers in a number of domains, including photocatalytic performance, gas sensors, glucose sensors, and solar cells. All things considered; Ce_2/Zr_2O_7 metal oxide nanocomposites are superior photocatalysts.

The development of innovative and efficient nanocomposite materials is becoming more and more crucial due to the product's favourable environmental effects. The degradation of methylene blue dye under solar radiation was evaluated in this work using ZrO_2 and AC/$Ce_2Zr_2O_7$ and the obtained data was examined and analyzed.

Experimental

The required chemicals in this study were Zirconyl nitrate ($Zr(NO_3)_2$. $3H_2O$), Cerium nitrate ($Ce(NO_3)_2$), oxalic acid and activated carbon all of which were analytical grade and used without further purification.

Green synthesis of zirconium oxide nanoparticles

In order to carry out a green synthesis of ZrO_2, 2.61g of zirconium nitrate trihydrate ($Zr(NO_3)_2$. $3H_2O$) and 0.24g of NaOH and 1.8g of plant extract were added to 70 ml of distilled water. The mixture was then stirred with a magnetic stirrer for 30 minutes at room temperature in order to maintain a pH of 7[2]. The mixture was poured into a 150 ml beaker and heated to 160°C for ten hours. Following the sample's return to room temperature, distilled water and ethanol were used to wash it. In a hot air oven, the product was dried at 80°C[3].

Journal of Chemical Health Risks

www.jchr.org

JCHR (2025) 15(6), 3739-3745 | ISSN:2251-6727

Green Synthesis of AC/$Ce_2Zr_2O_7$ nanocomposite

The AC/$Ce_2Zr_2O_7$ nanocomposite was created by dissolving 1.74g of zirconium nitrate trihydrate ($Zr(NO_3)_2.3H_2O$) in 40 ml of water, adding 0.12g of NaOH and Annona Squamosa L. peels extract (ASE) 2.1g to 20 ml of distilled water to keep the pH at 7, and agitating the mixture with a magnetic stirrer for 30 minutes at room temperature. 3g of purchased activated carbon Added to the reaction mixture[4,5]. The mixture was poured into a 150 ml beaker and heated to 160°C for ten hours. Following the sample's return to room temperature, ethanol and distilled water were used to wash it. In a hot air oven, the product was dried overnight at 80°C.

Characterization of AC/Ce_2/Zr_2O_7 nanocomposite

XRD Analysis

The XRD patterns of the prepared samples after calcination at 500 °C were analyzed and the observed diffraction peaks at 2θ values of activated carbon were found at (002) and (100). The ZrO_2 nanoparticle were found in the planes of (111), (200), (222) and (131), respectively (**JCPDS Card No. 79-1796**)[6,7]. AC/$Ce_2Zr_2O_7$ nanoparticles are ascribed to the corresponding planes of (002), (200), (110), (222), (311) and (131) confirmed the formation and well matched with **JCPDS Card No. 52-1104**[8]. These phenomena indicate that the formation of ZrO_2 and AC/$Ce_2Zr_2O_7$ nanocomposite began at the calcination temperature of about 450 °C. Peaks are not detected in other phases, indicating the high purity of the products shown in **(Fig.1)**[9]. Crystallite size of ZrO_2 and AC/$Ce_2Zr_2O_7$ nanocomposite were calculated by using Debye–Scherrer formula (Equation 1) and the values were presented in **Table 1.**

Debye–Scherer's equation

$$\text{Crystalline size (D)} = \frac{0.9\lambda}{\beta \cos\theta} \quad \text{------ (1)}$$

Where λ is the wavelength (λ = 1.5406 Å (Cu Kα), β is the full width half maximum (FWHM) and θ is the diffraction angle.

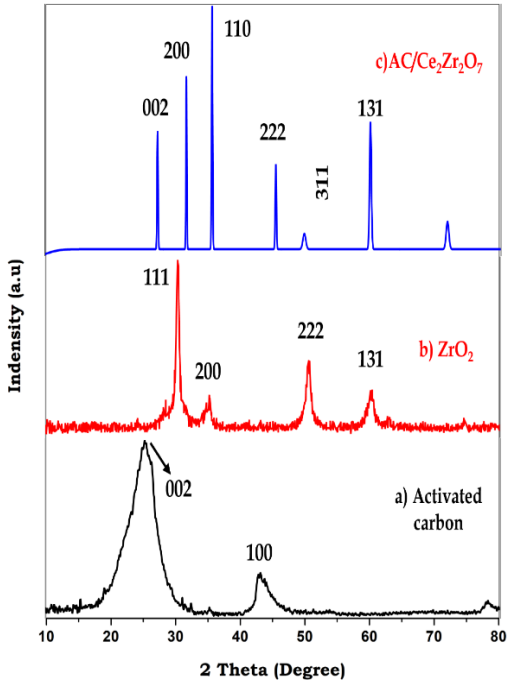

Fig.1 XRD spectra of a) Activated carbon, b) ZrO_2, c) AC/$Ce_2Zr_2O_7$ nanocomposite

Table.1. Crystalline size of (a) Activated carbon, b) ZrO_2 and AC/$Ce_2Zr_2O_7$ nanocomposite

S.No	Sample	Crystaline Size(nm)
1.	Activated carbon	24.2
2.	ZrO_2	29.4
3.	AC/Ce_2/Zr_2O_7	36.7

FT-IR Spectrum of AC/$Ce_2Zr_2O_7$ nanocomposite

Analyzing the various functional groups including oxygen-containing functional groups found in metal oxides is made easier with the use of the FT-IR approach. The stretching vibrations of activated carbon as present figure.2. ZrO_2, as seen in Fig. 2b FT-IR spectra, are centered at 562 cm^{-1} due to Zr-O stretching vibrations; the stretching vibrations of C–O and C=O groups found in metal oxide nanoparticles are represented by the peak at 1108 cm^{-1}, while the stretching vibrations of H–O–H are indicated by the peak at 3435 cm^{-1}[11]. The

Journal of Chemical Health Risks

www.jchr.org

JCHR (2025) 15(6), 3739-3745 | ISSN:2251-6727

stretching mode of the M-O bond is responsible for the stretching vibration peaks at 536 cm^{-1} (Figs. 2b and 2c); the stretching of the C–O and C=O groups present in the metal oxide nanoparticles is shown by the stretching vibration peak at 1178 cm^{-1}[12]. The H-O-H stretching vibrations are shown by the peaks at 3450, 3435 and 3425 cm^{-1}. Because it inhibits charge carrier fusion and has a synergistic effect that increases the nanocomposite's catalytic activity.

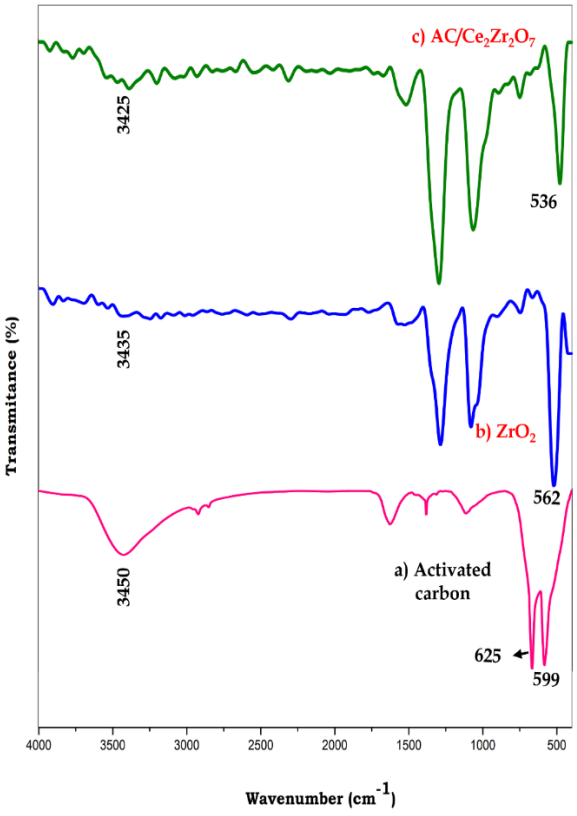

Fig. 2. FT-IR Spectrum of a) Activated carbon, b) ZrO_2, c) $AC/Ce_2Zr_2O_7$ nanocomposite

Morphology Analysis of $AC/Ce_2Zr_2O_7$ nanocomposite

Using SEM micrographs, the surface morphology of the synthesized Activated carbon, ZrO_2 and $AC/Ce_2Zr_2O_7$ nanocomposite was examined. The results are shown in Figs. 3a,3b and 3c. Figure 3a is showed sheet like structed activated carbon[13]. Figure 3b depicts the agglomerated structure of the ZrO_2 nanoparticle, whereas Figure 3b shows the uneven form of the ZrO_2 nanoparticles[14,15]. $AC/Ce_2/ZrO_2O_7$ nanocomposite were interestingly spherical in various directions[16].

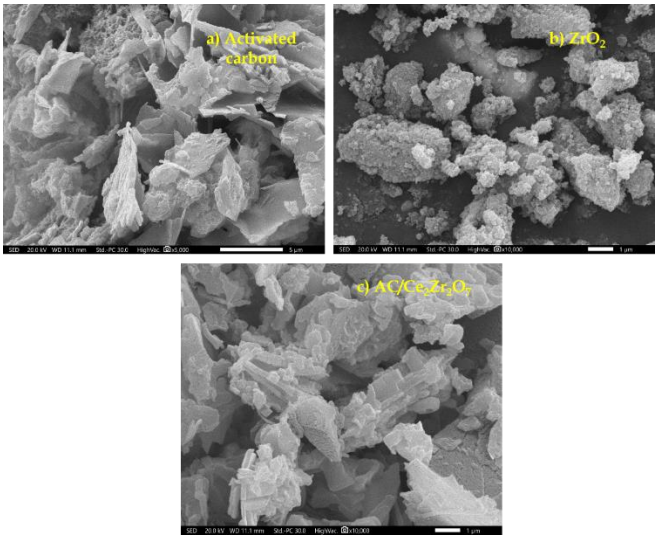

Fig.3 SEM analysis of a) Activated carbon, b) ZrO_2 c) $AC/Ce_2Zr_2O_7$ nanocomposite

Elemental Analysis of ZrO_2, Sn/ZrO_4 and Ce_2/ZrO_2O_7 nanocomposite

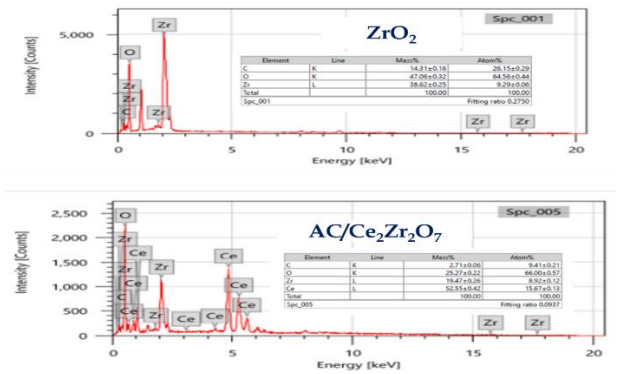

UV - DRS Analysis of Sn/ZrO_4 and Ce_2/Zr_2O_7 nanocomposite

Figure 4 displays the results of UV-diffuse reflectance spectroscopy of ZrO_2 and $AC/Ce_2Zr_2O_7$ nanocomposites. The results demonstrate that the UV absorption edge of the pure ZrO_2 and $AC/Ce_2Zr_2O_7$ nanocomposites was significantly noticed at 200 to 800 nm[17]. However, some samples' UV absorption migrated to the higher wavelength side. The band structure alterations are reflected in the variations in the absorption edges. Additionally, the equation for the Kubelka-Munk function is used to compute the bandgap of samples[18].

Journal of Chemical Health Risks

www.jchr.org

JCHR (2025) 15(6), 3739-3745 | ISSN:2251-6727

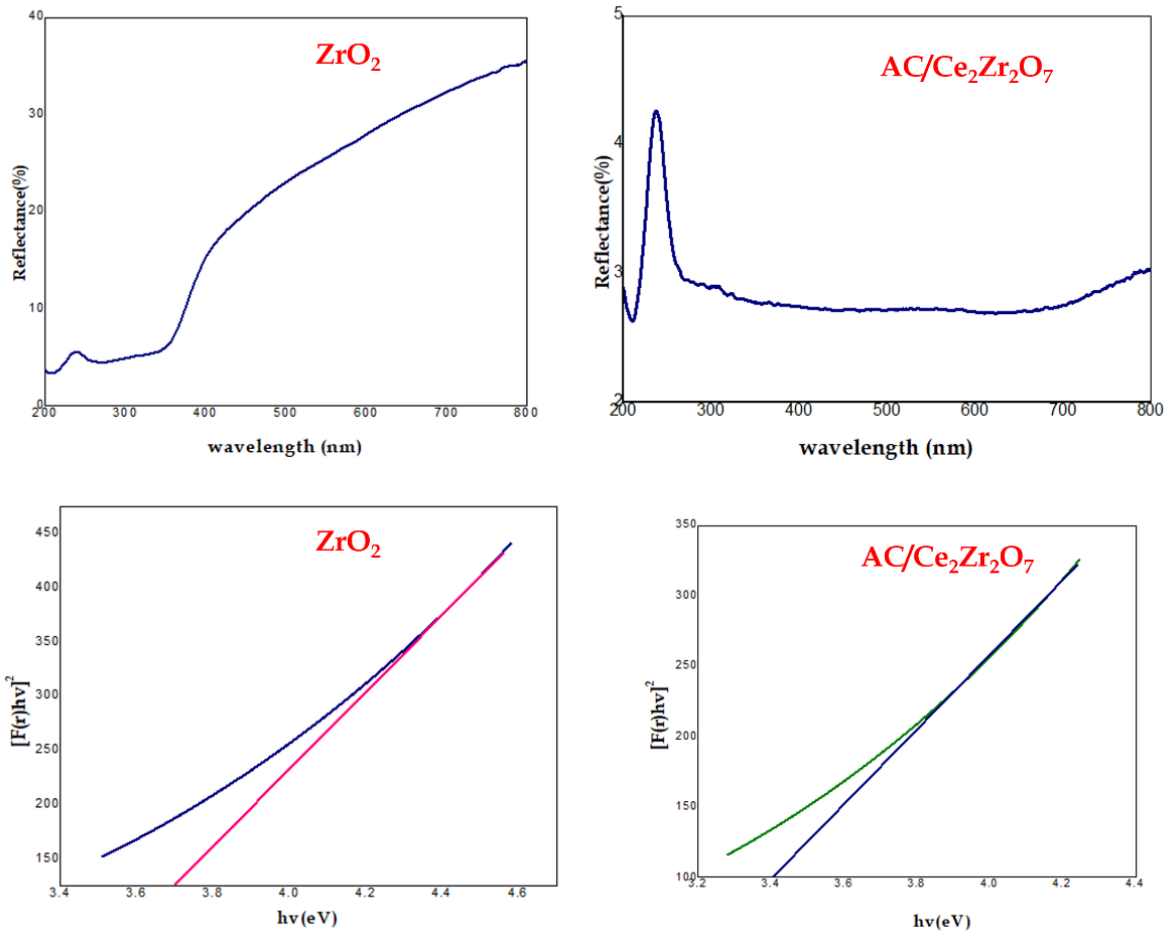

Fig. 4. UV-DRS Image of a) ZrO_2 b) $AC/Ce_2/Zr_2O_7$ c) Tauc's plot of ZrO_2 and d) Tauc's plot of $AC/Ce_2/Zr_2O_7$

$$\alpha h\nu = A\,(h\nu - E_g)n \quad \text{------ (2)}$$

Where α is the absorption coefficient and hν is the incident photon energy. As shown in **Fig.5**, the bandgap energies are estimated from the intercept of the tangents. The band gap of prepared ZrO_2 and $AC/Ce_2Zr_2O_7$ nanocomposites were found to be 3.7 and 3.4 eV respectively[19].

Photocatalytic Measurements

The degradation of methylene blue dye solutions, a model organic pollutant, was used to assess the photocatalytic activity efficiency of produced ZrO_2 and $AC/Ce_2Zr_2O_7$ nanocomposite under visible light and sunshine, respectively.

In under 60 minutes, the dye breakdown process utilizing solar radiation was completed (Fig. 5). In comparison to ZrO_2 catalyst, the produced $AC/Ce_2Zr_2O_7$ nanocomposite has demonstrated a quicker rate of dye degradation[20]. Figure 5a clearly illustrates the ZrO_2 nanocomposite's 72.7% methylene blue degradation efficiency, while Figure 5b displays the $AC/Ce_2Zr_2O_7$ nanocomposite's 88.2% methylene blue degradation efficiency after 60 minutes of sunshine irradiation[20].

Journal of Chemical Health Risks

www.jchr.org

JCHR (2025) 15(6), 3739-3745 | ISSN:2251-6727

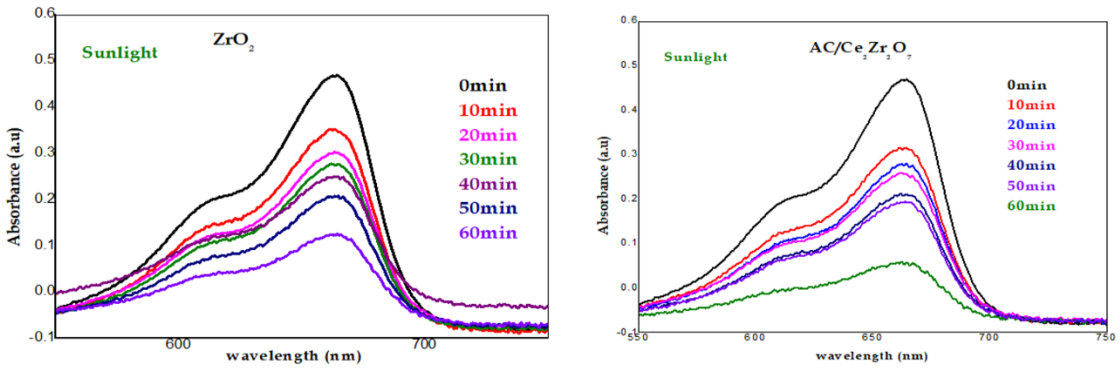

Fig. 5. UV-Vis spectra of ZrO_2 and $AC/Ce_2Zr_2O_7$ under sunlight irradiation.

The effectiveness of the nanocomposites' degradation was measured in weight percentages using 20 mg of catalyst. The breakdown efficiency of the produced materials under solar radiation is demonstrated in Figs. 6a and 6b, where it is found that $AC/Ce_2Zr_2O_7$ is more efficient than ZrO_2. Every ten minutes, the degradation efficiency was measured, allowing us to deduce that, when exposed to sunlight, the $AC/Ce_2Zr_2O_7$ composite material was more efficient than the ZrO_2 nanoparticles[21,22].

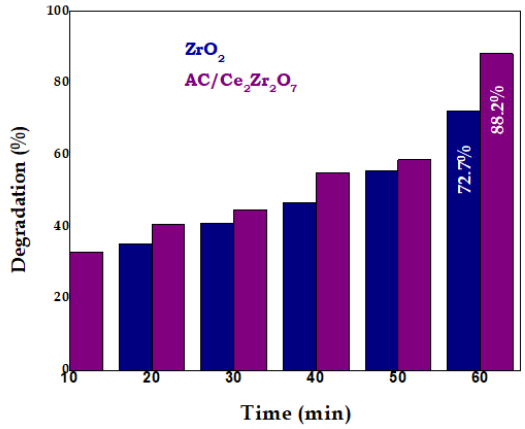

Fig.6. Photocatalytic degradation efficiency of methylene blue dye by using 20mg of catalyst under sunlight irradiation.

Mechanisms of photocatalysis:

The actual process of methylene blue dye degradation indicates that conduction band electrons (e-) and valence band holes (h+) are created when ZrO_2 and $AC/Ce_2Zr_2O_7$ nanoparticles were exposed to light energy bigger than or equal to their band gap energy. Organic compound oxidation is mediated by the creation of hydroxyl radicals, while reduction and oxidation processes are mediated by the production of superoxide radicals. A schematic illustration of the degradation mechanism is shown in Fig.7. Heterogeneous photocatalysis is produced through the oxidation pathway by the hydroxyl radical that is generated[23]. The dye may be reduced to superoxide radical $AC/Ce_2Zr_2O_7$ or photogenerated by combining electrons with electron acceptors such as O_2 that is dissolved in water or adsorbed on surfaces. When the photogenerated holes react with OH- or H_2O, they can oxidize organic molecules by generating ·OH radicals[24]. The majority of methylene blue may be oxidized by the OH radical into non-toxic byproducts such as, CO_2, H_2O, and mineralized product since it is such a potent oxidizing agent.

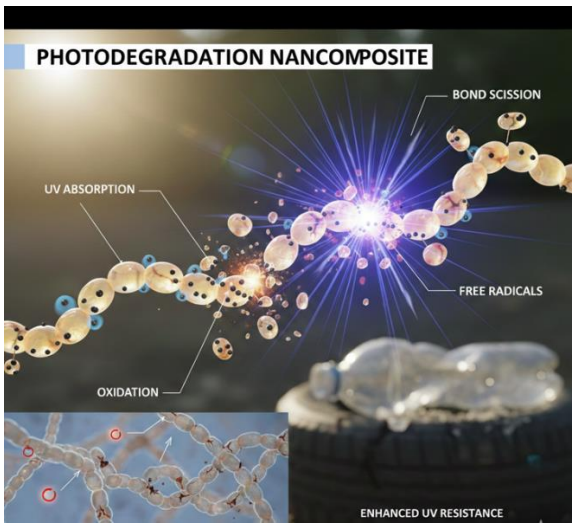

Fig.7. Mechanisms of photodegradation

Journal of Chemical Health Risks

www.jchr.org

JCHR (2025) 15(6), 3739-3745 | ISSN:2251-6727

Conclusion

The green synthesis approach was employed to synthesize the nanomaterials viz., ZrO_2 and $AC/Ce_2Zr_2O_7$ and were calcined at 450 °C for 6 hours, producing ZrO_2 and $AC/Ce_2Zr_2O_7$ nanomaterials with a crystalline size of 24.2, 29.4 and 36.7 nm with the agglomerated matrix and irregular structures. Kubelka-Munk function plot scrutinized that the band gap of ZrO_2 was 3.7 and $AC/Ce_2Zr_2O_7$ was 3.4 eV, respectively. The photocatalytic performance of the synthesized ZrO_2 and $AC/Ce_2Zr_2O_7$ nanocomposites against methylene blue dye was evaluated by sunlight irradiation with 20mg of weight percentages of the catalyst $AC/Ce_2Zr_2O_7$ nanomaterial showed a high degradation property (88.2%) compared to ZrO_2 materials (72.7%). The sunlight irradiation is a preferable source for eco-friendly photocatalytic degradation processes. The materials were also used for reducing the water pollution via an efficient photodegradation process.

Reference:

1. Chu, M. N., Nguyen, L. T., Truong, M. X., Do, T. H., Duong, T. T. A., Nguyen, L. T., & Pham, V. H. (2022). Ce^{3+}/Ce^{4+}-Doped ZrO_2/CuO nanocomposite for enhanced photocatalytic degradation of methylene blue under visible light. *Toxics*, *10*(8), 463.
2. Maulidya, A., Yulizar, Y., Bakri, R., Apriandanu, D. O. B., & Surya, R. M. (2022). Synthesis and characterizations of $Ce_2Zr_2O_7$–TiO_2 for increased photocatalytic activity toward degradation of methylene blue. *Ceramics International*, *48*(19), 29523-29532.
3. Bakkiyaraj, R., Balakrishnan, M., Bharath, G., & Ponpandian, N. (2017). Facile synthesis, structural characterization, photocatalytic and antimicrobial activities of Zr doped CeO_2 nanoparticles. *Journal of Alloys and Compounds*, *724*, 555-564.
4. Meena, S., Anantharaju, K. S., Vidya, Y. S., Renuka, L., Malini, S., Sharma, S. C., & Nagabhushana, H. (2020). $MnFe_2O_4/ZrO_2$ nanocomposite as an efficient magnetically separable photocatalyst with good response to sunlight: Preparation, characterization and catalytic mechanism. *SN Applied Sciences*, *2*, 1-12.
5. Meena, S., Anantharaju, K. S., Vidya, Y. S., Renuka, L., Malini, S., Sharma, S. C., & Nagabhushana, H. (2020). $MnFe_2O_4/ZrO_2$ nanocomposite as an efficient magnetically separable photocatalyst with good response to sunlight: Preparation, characterization and catalytic mechanism. *SN Applied Sciences*, *2*, 1-12.
6. Hokonya, N., Mahamadi, C., Mukaratirwa-Muchanyereyi, N., Gutu, T., & Zvinowanda, C. (2022). Green synthesis of P− ZrO_2CeO_2ZnO nanoparticles using leaf extracts of Flacourtia indica and their application for the photocatalytic degradation of a model toxic dye, Congo red. *Heliyon*, *8*(8).
7. Li, P., Guo, M., Wang, Q., Li, Z., Wang, C., Chen, N., & Chen, S. (2019). Controllable synthesis of cerium zirconium oxide nanocomposites and their application for photocatalytic degradation of sulfonamides. *Applied Catalysis B: Environmental*, *259*, 118107.
8. Oppong, S. O. B., Opoku, F., Anku, W. W., Kiarii, E. M., & Govender, P. P. (2019). Experimental and computational design of highly active Ce–ZrO_2–GO photocatalyst for eosin yellow dye degradation: the role of interface and Ce^{3+} ion. *Catalysis Letters*, *149*, 1633-1650.
9. Zinatloo-Ajabshir, S., Morassaei, M. S., & Salavati-Niasari, M. (2017). Facile fabrication of $Dy_2Sn_2O_7$-SnO_2 nanocomposites as an effective photocatalyst for degradation and removal of organic contaminants. *Journal of colloid and interface science*, *497*, 298-308.
10. Sutar, R. S., Barkul, R. P., & Patil, M. K. (2021). Visible light assisted photocatalytic degradation of methylene blue dye and mixture of dyes using ZrO_2-TiO_2 nanocomposites. *Current Nanoscience*, *17*(1), 120-129.
11. Meena, S., Anantharaju, K. S., Vidya, Y. S., Renuka, L., Malini, S., Sharma, S. C., & Nagabhushana, H. (2020). $MnFe_2O_4/ZrO_2$ nanocomposite as an efficient magnetically separable photocatalyst with good response to sunlight: Preparation, characterization and catalytic mechanism. *SN Applied Sciences*, *2*, 1-12.
12. Quang, D. A., Toan, T. T. T., Tung, T. Q., Hoa, T. T., Mau, T. X., & Khieu, D. Q. (2018). Synthesis of CeO_2/TiO_2 nanotubes and heterogeneous photocatalytic degradation of methylene

Journal of Chemical Health Risks

www.jchr.org

JCHR (2025) 15(6), 3739-3745 | ISSN:2251-6727

blue. *Journal of environmental chemical engineering*, *6*(5), 5999-6011.

13. Thakur, M., Sharma, G., Ahamad, T., Ghfar, A. A., Pathania, D., & Naushad, M. (2017). Efficient photocatalytic degradation of toxic dyes from aqueous environment using gelatin-Zr (IV) phosphate nanocomposite and its antimicrobial activity. *Colloids and Surfaces B: Biointerfaces*, *157*, 456-463.
14. Sayed, M. A., Abo-Aly, M. M., Aziz, A. A. A., Hassan, A., & Salem, A. N. M. (2021). A facile hydrothermal synthesis of novel CeO_2/CdSe and CeO_2/CdTe Nanocomposites: Spectroscopic investigations for economically feasible photocatalytic degradation of Congo red dye. *Inorganic Chemistry Communications*, *130*, 108750.
15. Kumar, O. P., Ashiq, M. N., Shah, S. S. A., Akhtar, S., Obaidi, M. A. A., Mujtaba, I. M., & ur Rehman, A. (2021). Nanoscale ZrRGOCuFe layered double hydroxide composites for enhanced photocatalytic degradation of dye contaminant. *Materials Science in Semiconductor Processing*, *128*, 105748
16. Munawar, T., Mukhtar, F., Nadeem, M. S., Riaz, M., ur Rahman, M. N., Mahmood, K., & Iqbal, F. (2020). Novel photocatalyst and antibacterial agent; direct dual Z-scheme ZnO–CeO_2-Yb_2O_3 heterostructured nanocomposite. *Solid State Sciences*, *109*, 106446.
17. Najjar, M., Hosseini, H. A., Masoudi, A., Sabouri, Z., Mostafapour, A., Khatami, M., & Darroudi, M. (2021). Green chemical approach for the synthesis of SnO_2 nanoparticles and its application in photocatalytic degradation of Eriochrome Black T dye. *Optik*, *242*, 167152.
18. Gusain, R., Gupta, K., Joshi, P., & Khatri, O. P. (2019). Adsorptive removal and photocatalytic degradation of organic pollutants using metal oxides and their composites: A comprehensive review. *Advances in colloid and interface science*, *272*, 102009.
19. Siddiqui, S. I., Manzoor, O., Mohsin, M., & Chaudhry, S. A. (2019). Nigella sativa seed-based nanocomposite-MnO_2/BC: An antibacterial material for photocatalytic degradation, and adsorptive removal of Methylene blue from water. *Environmental research*, *171*, 328-340.
20. Karuppusamy, I., Samuel, M. S., Selvarajan, E., Shanmugam, S., Kumar, P. S. M., Brindhadevi, K., & Pugazhendhi, A. (2021). Ultrasound-assisted synthesis of mixed calcium magnesium oxide ($CaMgO_2$) nanoflakes for photocatalytic degradation of methylene blue. *Journal of Colloid and Interface Science*, *584*, 770-778.
21. Oppong, S. O. B., Opoku, F., Anku, W. W., Kiarii, E. M., & Govender, P. P. (2019). Experimental and computational design of highly active Ce–ZrO_2–GO photocatalyst for eosin yellow dye degradation: the role of interface and Ce^{3+} ion. *Catalysis Letters*, *149*, 1633-1650.
22. Gionco, C., Hernández, S., Castellino, M., Gadhi, T. A., Muñoz-Tabares, J. A., Cerrato, E., & Paganini, M. C. (2019). Synthesis and characterization of Ce and Er doped ZrO_2 nanoparticles as solar light driven photocatalysts. *Journal of Alloys and Compounds*, *775*, 896-904.
23. Meena, S., Anantharaju, K. S., Vidya, Y. S., Renuka, L., Malini, S., Sharma, S. C., & Nagabhushana, H. (2020). $MnFe_2O_4$/ZrO_2 nanocomposite as an efficient magnetically separable photocatalyst with good response to sunlight: Preparation, characterization and catalytic mechanism. *SN Applied Sciences*, *2*, 1-12.
24. Manibalan, G., Murugadoss, G., Thangamuthu, R., Kumar, R. M., Jayavel, R., & Kumar, M. R. (2019). Enhanced photocatalytic performance of heterostructure CeO_2–SnO_2 nanocomposite via hydrothermal route. *Materials Research Express*, *6*(7), 075032.